JOURNAL OF PROPULSION AND POWER
Vol. 11, No. 4, July–August 1995

Development of Gas-Phase Reaction Mechanisms for Nitramine Combustion

R. A. Yetter,* F. L. Dryer,† M. T. Allen,‡ and J. L. Gatto‡
Princeton University, Princeton, New Jersey 08544

A methodology for developing gas-phase reaction mechanisms for nitramine propellants is discussed. Examples of fundamental kinetic experiments and detailed modeling calculations are given that emphasize a hierarchical construction procedure for both the types of experiments necessary for collecting kinetic data and the specific chemical submodels that need to be studied. In particular, three kinetic submodels of increasing complexity are described with selected results from flow reactor experiments. With kinetic data generated from these experiments and others, chemical submodels are developed and validated by comparison of model predictions with experimental measurements using reaction flux and sensitivity analyses to guide the process. Collectively, the submodels, validated over the entire range of experimentally studied conditions, are assembled to form the gas-phase nitramine combustion mechanism. Because of the nature of the developmental procedure, e.g., the necessity for different types of experiments, ranging from "microscopic" measurements of isolated reaction rate constants to "macroscopic" studies on kinetic mechanisms in flames, the process is inherently iterative. As an example of this iterative procedure, numerical results are presented on the ignition behavior of hexahydro-1,3,5-trinitro-1,3,5-triazine (RDX) after updating a previously developed model with recent results from submodel validation experiments. These results show changes in the pathways of many secondary species involved in RDX decomposition.

Introduction

NEWLY developed energetic polycyclic nitramines and energetic polymers have the potential to offer significant energy density and plume signature advantages over current state-of-the-art propellants in strategic, tactical rocket, and gun propulsion. Current state-of-the-art propellants, such as octahydro-1,3,5,7-tetranitro-1,3,5,7-tetrazocine (HMX) and hexahydro-1,3,5-trinitro-1,3,5-triazine (RDX), were developed empirically over a lengthy period of time, being first synthesized nearly a century ago. The development and implementation of the next generation of propellants will have to meet new and more stringent requirements of energy density, burn rate, stability, signature, and hazards specifications, and formulations will likely be based on combinations of more than 10 new oxidizers and energetic polymers. Fundamental to the understanding of and ability to predict propellant combustion phenomena is a quantitative understanding of the elementary chemical and physical processes in the gas, liquid, and solid phases of propellant ignition and combustion.

In the past, the development of propellant formulations has largely been empirically based with regard to combustion performance. With recent advances in the combustion sciences, mainly as a result of new diagnostic techniques and larger/faster computers, it now appears feasible and desirable to use fundamentally based models for aiding the development of propellant formulations. Overviews of such a program have recently been described in the literature.[1-3]

As in the development of all complex models, it is advantageous to divide a model into submodels that can be developed and validated separately, thus reducing the complexity of the process. A natural subdivision for a general propellant combustion model is to separately construct and validate submodels for the gas-phase and condensed-phase processes as shown in Fig. 1.

Research on the gas-phase is important because it generally produces the bulk of the energy release and establishes both the thermal and concentration gradients at the burning propellant surface. Basic understanding of the gas-phase process (Fig. 2) starts with knowledge of the thermochemical, kinetic, and transport properties of key nitramine species, and ends with the validation of a comprehensive mechanism for the gas-phase reaction of decomposition products from the propellant surface. In this hierarchical approach, theory at the most fundamental level and at a semi-empirical level interact with laboratory measurements of rate constants, product pathways, and transport properties. From these pieces of information, a well-founded chemical mechanism with associated rate constants is first derived and validated by comparisons of model prediction with kinetic data from shock tubes, flow reactors, and static reactors. With the development of a "pure" chemistry model accomplished, the effects of heat release and species/energy transport are included by simula-

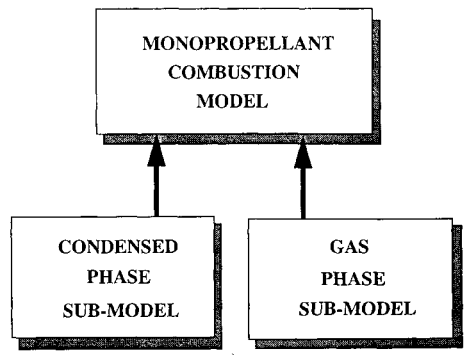

Fig. 1 Propellant combustion model development.

Received Sept. 21, 1994; revision received Feb. 6, 1995; accepted for publication Feb. 6, 1995.

*Research Scientist and Correspondent, Department of Mechanical and Aerospace Engineering.
†Professor, Department of Mechanical and Aerospace Engineering.
‡Research Assistant, Department of Mechanical and Aerospace Engineering.

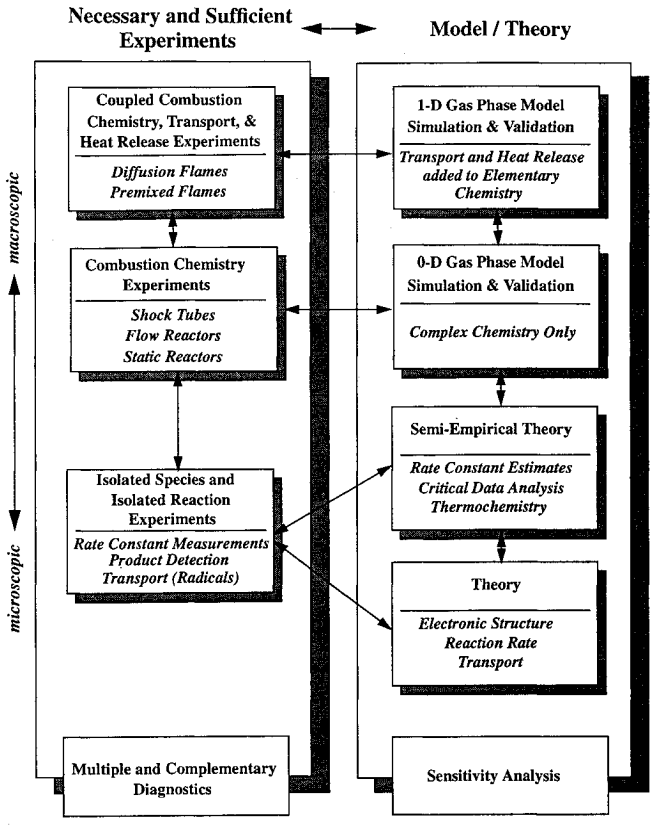

Fig. 2 Nitrogen combustion chemistry and transport network validation.

tion and validation of premixed and diffusion flames. Sensitivity analysis techniques are required at each level of theory and model development and validation. In particular, sensitivity analysis allows a natural link between experimental and modeling efforts and can be used, e.g., to design experiments or to identify key species and reactions that require further theoretical study. Finally, multiple and complementary diagnostic techniques are essential to each of the experimental programs, not only to provide internal consistency checks, but also to provide a sufficient amount of information to severely constrain the parameters of the associated model.

The assembly and validation of detailed kinetic mechanisms are important aspects of developing an understanding of the chemical processes occurring in propellant combustion. The resulting mechanisms provide useful tools in determining what elementary reactions require improved definition, in acting as benchmarks against which simplified (reduced or lumped) chemistry models can be developed and tested, and in evaluating the interactions of chemistry and transport phenomena in simple one-dimensional systems. Moreover, comprehensive mechanisms, evaluated and validated over larger ranges in pressure, temperature, and equivalence ratio are required for simulating the more practical combustion environments where gas-phase chemistry is intimately coupled with chemical processes occurring at the material surface. Unfortunately, mechanistic kinetic data are presently not attainable for all the conditions of practical interest, e.g., very high pressures, and therefore, it is often desirable that a comprehensive mechanism predict, with some degree of confidence, the kinetic behavior of systems for which confirmation data are not available. This condition is generally valid when the kinetics to be predicted fall within the boundaries for which the mechanism has been validated. However, outside this region of calibration, predictions from comprehensive reaction mechanisms should be used cautiously.

In this article, the principle of hierarchical model development and validation is applied to the construction and further refinement of a gas-phase reaction mechanism for RDX combustion. As one necessary component of this process, results from kinetic experiments conducted in a variable temperature, variable pressure flow reactor on several chemical submodels of different complexity, are presented. This work represents an initial and important step in extending the pressure range of mechanistic kinetic data above atmospheric pressure at intermediate temperatures. Finally, calculations on the ignition kinetics of RDX are analyzed and compared for two RDX models; the original model of Melius[4] and a revised model based on recent chemical submodel development and validation.

Mechanism Development and Validation

Reaction mechanisms can be developed systematically,[5] beginning with the simplest species and reactions that are common subelements in the combustion of more complex species, and sequentially constructed by incorporating new species and reactions in order of increasing complexity. At each level, the newly added portions of the mechanism must be tested and validated by thorough comparison between numerically predicted and experimentally observed results. However, because of the sequential ordering, only those features that have been added need to be examined closely. This process is given further order by identification of the important features through application of sensitivity analysis and reaction pathway techniques.

The validation at each level of development of a reaction mechanism requires experimental data from several sources such as shock tubes, flow reactors, and static reactors. It is not sufficient to test a mechanism by comparison with a single experiment, because different elementary reactions can be dominant under different experimental conditions. Furthermore, no single kinetics experiment covers the entire range of pressure/temperature/residence time parameters that is important under combustion conditions. Some reactions are negligible except under high-temperature shock-tube conditions, while others become unimportant for temperatures above 1000 K. Unless a mechanism is to be used only for a restricted class of applications under a specific set of system parameters, it must be validated by comparison with experimental data over wide ranges of physical conditions.

The three experiments mentioned above decouple chemistry from transport phenomena and excessive heat release rates, and provide mechanistic kinetic data for different time scales of reaction. Typically, shock tubes cover 1–1000 μs and, hence, are used to study high-temperature kinetics ($T > 1000$ K). Flow reactors have time scales typically between 10–1000 ms and are used to study kinetics at intermediate temperatures (600 K $< T <$ 1200 K), while static reactors have a time scale between 0.1–1000 s and are used to study kinetics at low temperatures ($T < 800$ K). Variations in pressure also affect the accessible residence time/temperature ranges of each of these experiments and can often be used to extend these ranges.

An important component to the process of mechanism development, not discussed here, is the experimental and theoretical studies on individual species and reactions, described in the bottom half of Fig. 2. Such studies provide the elemental parameter input necessary for mechanism development. These two types of kinetic studies, i.e., those devoted to complex mechanisms and those devoted to isolated reactions, must be conducted interactively for efficient and successful model development. For example, the rates of all possible elementary reactions cannot be practically measured in the laboratory; however, mechanistic studies combined with sensitivity analysis may be used to pinpoint and place priority on those individual reactions that require the most attention. A particularly important component of model development, which cannot be overstated here (which frequently is not recognized as crucial), is the continued updating of databases from critical

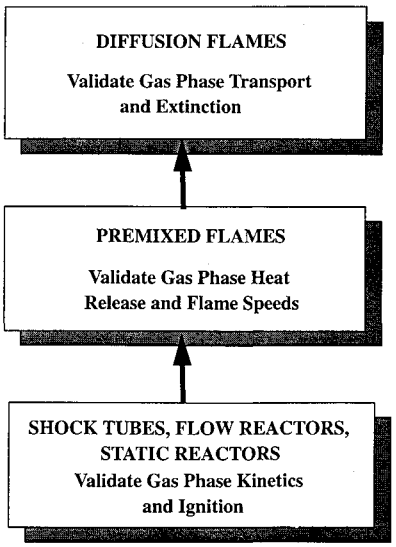

Fig. 3 Hierarchical development and validation of gas-phase submodels.

reviews. One should also not construe that the development and critical assessment of elementary databases can substitute for systems model development and validation. Uncertainties associated with the elementary parameters are often large enough to cause significant variations in the predictions of systems behaviors.[6]

Once a homogeneous gas-phase kinetics model has been developed, validation of coupled gas-phase heat release rates and gas-phase transport is required to complete the development and validation of the entire gas-phase thermochemical, kinetic, and transport model. The procedure is again hierarchical and is shown schematically in Fig. 3. Data from premixed flames are necessary to validate heat release rates and flame speed predictions. In premixed flames, kinetics and transport are of almost equal importance; however, the system is almost entirely driven by the heat release and, hence, the temperature profile through the flame. The ability to deconvolute the kinetics, which produce this heat release, is very difficult due to simultaneous transport processes and the high sensitivity of measured observables to the temperature measurements. Data from diffusion flames are necessary to validate transport and extinction phenomena, in addition to gas-phase kinetics and heat release rates.

The chemical submodels that need to be studied and developed will, of course, depend upon the propellant of interest. For the remainder of this article, model development will focus around RDX. However, as will be shown in the next section, the chemical submodels developed and validated for RDX will also have commonality to many different types of propellants.

RDX Flame Structure

An important experimental flame study on the gas-phase speciation above deflagrating RDX was performed by Korobeinichev and co-workers.[7–9] Their study with mass spectrometer probe measurements identified HCN as a primary product of decomposition. Earlier studies[10–12] had proposed mainly gas-phase products of CH_2O, CO, CO_2, H_2O, NO, NO_2, N_2, and N_2O. From the detailed studies of Korobeinichev and co-workers, the overall reaction for gas-phase decomposition of RDX at 0.5 atm was determined to be

$$\text{RDX} \rightarrow 0.244H_2O + 0.078N_2 + 0.238NO + 0.044N_2O + 0.024NO_2 + 0.044CO + 0.069CO_2 + 0.238HCN + 0.024HNCO$$

From energy balance considerations, Korobeinichev et al. confirmed that a narrow surface zone exists where RDX vapor can decompose. More importantly, these studies also produced species profiles as a function of position above the surface showing in detail the reaction sequence from the vapor phase decomposition products of RDX to final equilibrium gas-phase products (CO, CO_2, H_2, H_2O, and N_2). More recent studies on the speciation of gas-phase species above burning RDX have been performed by Fetherolf and Litzinger[13] and Hanson–Parr and Parr.[14,15] The experimental work of Fetherolf and Litzinger is similar to that of Korobeinichev et al. Using microprobe/mass spectrometer measurements of laser-assisted combustion of RDX at 0.5 atm, Fetherolf and Litzinger found the following composition at the surface:

$$\text{RDX} \rightarrow 0.145H_2O + 0.12N_2 + 0.11NO + 0.08N_2O + 0.13NO_2 + 0.043CO + 0.01CO_2 + 0.187HCN + 0.17CH_2O + 0.005H_2$$

Hanson–Parr and Parr have studied gas-phase speciation above deflagrating RDX using nonintrusive optical diagnostic techniques. Measurements of NO, NO_2, CN, NH, CH_2O, and OH have been made using uv-visible absorption and planar laser-induced fluorescence. In addition, spectroscopic measurements of temperature were obtained, clearly showing the two-zone heat-release structure in the gas-phase. In contrast to the work of Fetherolf and Litzinger, formaldehyde was not detected in these experiments.

Collectively, these results show that NO_2, CH_2O, and HNCO (when observed), are consumed first, forming NO, H_2O, CO, CO_2, and H_2. A short distance downstream, N_2O is consumed forming N_2. Further downstream, HCN, NO, and some H_2O are consumed forming the remaining CO, CO_2, H_2, and N_2 to complete the reaction. Near the end of this reaction, a luminous flame develops where NH and CN appear and are consumed. At the same location, OH is formed and reaches a constant value. The zone between the consumption of NO_2 and CH_2O and the consumption of HCN and NO is often referred to as the "dark" zone in RDX deflagration.

Data from flame experiments have enabled the development of phenomenological and detailed models of the flame structure. Korobeinichev et al.[8,9] developed a model to describe the gas-phase kinetics starting with decomposition products and calculated the resulting profiles downstream. Melius[4,16,17] has developed a model to describe the entire decomposition process starting from RDX decomposition. Although much work has been devoted to the mechanisms of initial decomposition, considerable uncertainty still remains in the controlling pathways of importance to propellant flames. Figures 4 and 5 present a phenomenological mechanism for reaction in the first stage based on current literature. The initial decomposition can occur by fission of a N—N bond followed by the unraveling of the remaining cyclic structure by breakage of C—N bonds, one bond removed from the newly created radical site.[16] Earlier studies have also considered direct HONO elimination.[18] More recently, concerted detrimerization has been shown to be the major decomposition pathway under isolated conditions using IR multiphoton dissociation.[19] Reactions for the consumption of methylenenitramine (Fig. 4) also require further study, although in general, its decomposition is felt to lead to the gas-phase branching ratio observed between HCN and NO_2 formation at higher temperatures (high heating rates) vs CH_2O and N_2O formation at lower temperatures (low heating rates). Water-assisted decomposition of H_2CNNO_2 has also been proposed to be important.[17] In addition to decomposition mechanisms for both RDX and methylenenitramine, bimolecular reactions also can be effective (Fig. 5), particularly in combustion systems once the radical pool has been initiated and also in

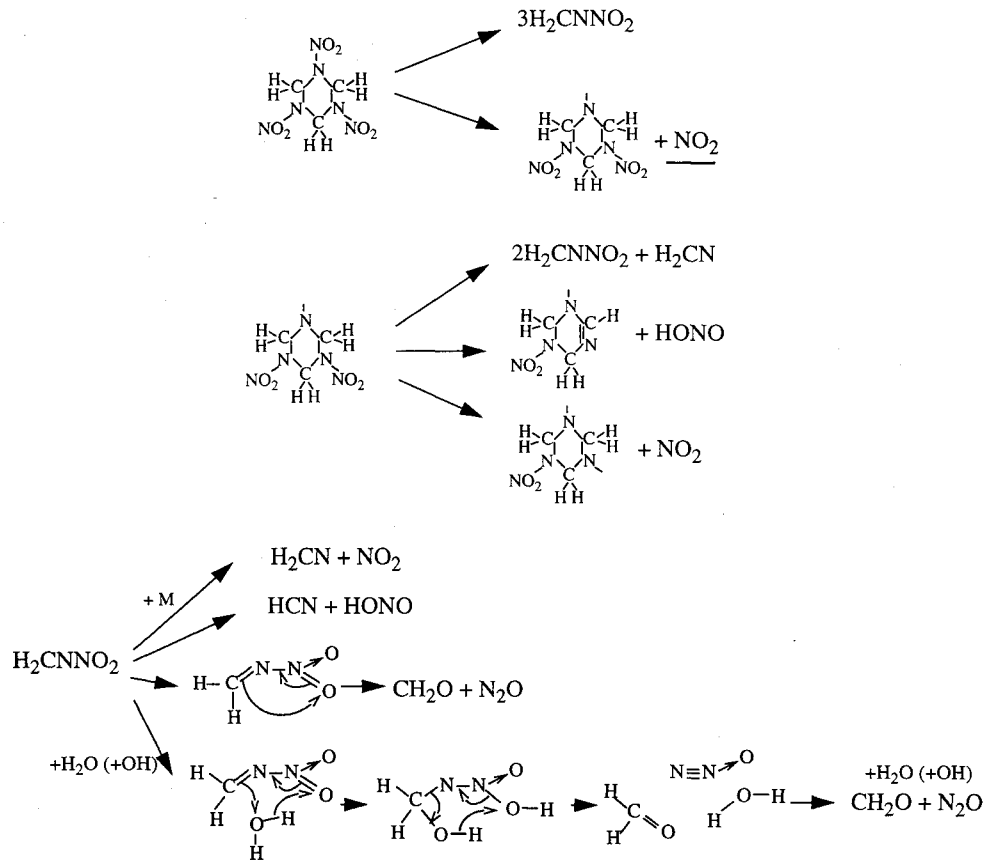

Fig. 4 Gas-phase RDX decomposition mechanism: primary decomposition steps.

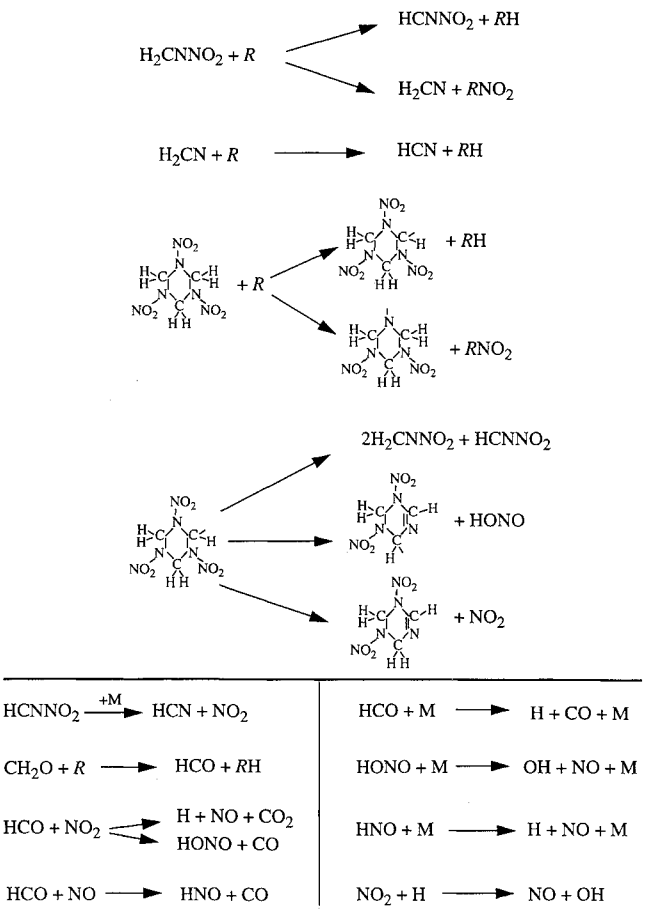

Fig. 5 Gas-phase RDX decomposition mechanism: decomposition of secondary products and secondary reactions.

systems where significant concentration gradients exist leading to molecular transport. Li and Williams[20] predict that a controlling bimolecular reaction is necessary in the initial decomposition to explain the pressure dependence (0.8) observed in the deflagration velocity of RDX.

The interpretation of gas-phase decomposition routes and products observed during deflagrating RDX is further complicated due to the possibility of simultaneous condensed-phase reactions leading to gas-phase products. Recent studies by Brill and co-workers[21–24] and Behrens and Bulusu[25–27] have revealed possible mechanisms occurring in the condensed-phase. In the T-jump experiments of Brill,[22] N_2O and NO_2 have been observed to precede evolution of all other gas-phase species from the surface of RDX. The ratio of N_2O to NO_2 was found to decrease with increasing temperatures, being approximately equal for temperatures of 570–620 K, which is near the surface temperature of a burning propellant. Although the ratio of CH_2O to HCN was not observed to follow this trend, both HCN and CH_2O, along with CO, CO_2, H_2O, HNCO, NO_2, N_2O, and NO have been measured as gas-phase products of condensed-phase processes. Behrens and Bulusu[26] have used simultaneous thermogravimetric modulated beam mass spectrometry to identify four primary condensed-phase decomposition pathways. They concluded that the decomposition mechanism must account for formation of oxy-*s*-triazine and 1-nitroso-3,5-dinitrohexahydro-*s*-triazine,[27] since the final products formed during decomposition may be formed via these intermediates.

It is evident from Figs. 4 and 5 (and also from the condensed-phase decomposition experiments) that the decomposition products measured experimentally in deflagrating RDX flames can all be accounted for on a phenomenological basis. Additional species such as CO and CO_2 can be explained by the further oxidation of CH_2O. The formation of H_2O and H_2 can be explained by hydrogen abstraction reactions of RDX and its secondary products via OH and H radical attack.

Formation of HONO can occur either by direct elimination or by reaction of NO_2 with RDX and secondary products. Finally, NO can be formed by HONO dissociation or from conversion of NO_2 to NO.

Hierarchical Chemical Systems

The decomposition products and species profiles from RDX flames suggest a natural subdivision of gas-phase chemical models as shown in Fig. 6. The approach to model construction flows in the opposite direction as the sequence of reaction. The first gas-phase models that need to be developed and validated are those for the decomposition of NO_2 and N_2O. Once these mechanisms are developed and validated, more complex chemical systems, beginning with H_2 and a nitrogen-containing oxidizer, can be studied. Because NO_2 leads to NO formation, one must also consider reaction systems with NO as the oxidizer. Continued development proceeds subsequently through CO oxidation, CH_2O oxidation, and HCN oxidation. Ammonia is a convenient source of NH_2 and NH radicals, both of which are important unstable intermediates in the oxidation and decomposition of nitramines. Since the development of one chemical submodel of greater complexity depends upon the development and validation of those simpler, once the simpler systems are developed and validated, the validation process in theory depends only on the parameters of the newly added reactions and species. In this way, model development is efficient and, more importantly, internally consistent. However, once a refinement occurs in a submodel, the validation process needs to be repeated beginning with the simplest submodel where the refinement occurred.

Each of these submodels is generated by the following approach:

1) Identify the important chemical species and determine their associated thermochemical parameters and corresponding uncertainties by literature review and/or parameter estimation.

2) Identify the important chemical reactions and determine their associated kinetic parameters and corresponding uncertainties by literature review and/or parameter estimation.

3) Calculate the time and spatial dependent solutions of species and temperature profiles and associated sensitivities.

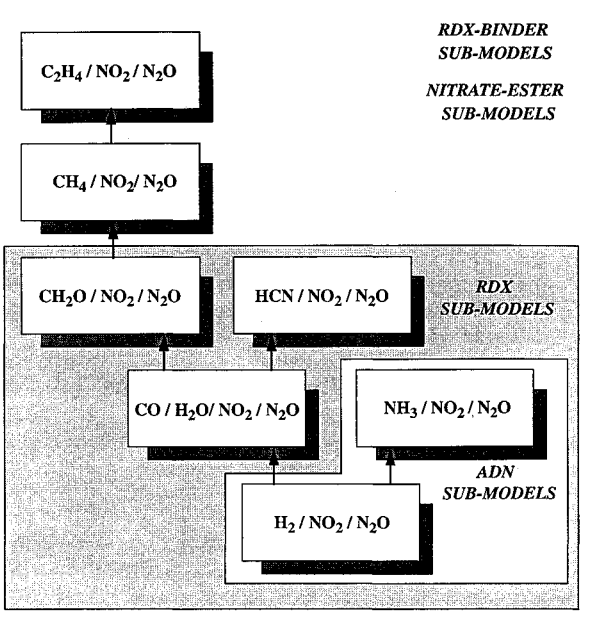

Fig. 6 Hierarchical development and validation of gas-phase reaction mechanisms. Note the commonality between different propellants and gas-phase submodels.

4) Measure or calculate (using fundamental theoretical methods) parameters that have simultaneously large sensitivities and large uncertainties.

5) Design experiments for both parameter measurement and systems validation.

6) Iterate through the above steps.

As a starting point to this approach, Tsang and Herron[28] have proposed a reaction grid for RDX combustion consisting of 38 species and over 700 possible interactions between the proposed species. Many of these interactions may be discarded based on thermochemical and structural considerations, significantly reducing the number of elementary reactions that need to be included.

Examination of Fig. 6 also illustrates another important benefit from the construction of hierarchical chemical systems. Note that the $H_2/NO_2/N_2O$ and $NH_3/NO_2/N_2O$ submodels also form the basis for a gas-phase model of ammonium dinitramide (ADN).[29,30] The primary surface reaction products observed from ADN consist of NH_3, N_2O, NO_2, H_2O, NO, N_2, HNO_3, and NH_4NO_3. The ammonium nitrate likely results from recombination of NH_3 and HNO_3 at low temperature.[30] In flames, it is less likely to form. However, HNO_3 is a likely product formed from the decomposition of $HN(NO_2)_2$ and is the only additional species that would need to be studied in the submodel hierarchy.

Ethylene and methane are selected in Fig. 6 to be representative of gas-phase intermediates produced from the combustion of energetic binders. Experimental results by Parr on polycyclic nitramine flames have indicated that the interaction between an energetic binder and the polycyclic nitramine can significantly affect the ignition and combustion characteristics. Consequently, an understanding of the gas-phase kinetics of binder intermediates, such as C_2H_4 and CH_4, is also important if a composite propellant model is to be developed. The methane reaction may be considered a submechanism of C_2H_4 by assuming that the dominant route for CH_3 radicals is reaction with NO_2 and not itself. However, under fuel-rich conditions, methyl radicals can be expected to recombine to form ethane, and hence, the hierarchical structure of Fig. 6 would have to be modified accordingly. Mixtures of paraffinic hydrocarbons with NO_2 also form the gas-phase models for the thermal decomposition of nitrate-esters.[31,32] For example, CH_4/NO_2 mixtures are submodels of nitromethane, methyl nitrite, or methyl nitrate, and C_2H_6/NO_2 mixtures are submodels of nitroethane or ethyl nitrate.

A significant amount of research exists in the literature on these submodels and is too vast to review here. Some recent examples of work in static reactors and shock tubes include those of Refs. 31, and 33–40. Examples of recent studies in premixed and diffusion flames include those of Refs. 41–50. Relevant kinetics research also exist in NO_x emissions problems in combustion. In these systems, the NO_x levels are typically small compared to the levels found in propellant combustion and significant amounts of molecular oxygen are present. A good review of this chemistry has been reported by Miller and Bowman.[51] In building a comprehensive mechanism, all relevant data need to be considered, with the goal that a single chemical model can predict the results collectively.

Chemical submodel development is illustrated here through a series of examples with flow reactor experiments. Flow reactor experiments are important in propellant combustion because the chemistry near the burning propellant surface is well within the temperature range of the flow reactor, and second, the high convective flows spread the reaction zone over approximately a meter in length, thus providing excellent spatial resolution from which to obtain accurate kinetic data. For example, the temperature and NO_2 concentration measurements of Hanson-Parr and Parr[14,15] for laser-assisted RDX deflagration at 1 atm show the temperature to rise from the surface temperature (~600 K) to the dark zone temperature

within approximately 0.2 mm. Nitrogen dioxide is formed and consumed all within about 1 mm. The 0.5-atm modeling calculations of RDX deflagration by Melius predicted consumption of NO_2, CH_2O, and HONO within 2 mm of the propellant surface and prior to the gas-phase temperature rising above 1200 K. The ability to obtain accurate kinetic data from such dimensions is currently limited.

Examples of Chemical Submodel Development with Flow Reactor Experiments

Flow reactor experiments are unique in providing experimental data in a range of conditions typically not accessible in shock tubes and static reactors, yet still of significant importance to propellant combustion. From such experiments, the evolution of stable reactants, intermediates, and product concentrations for chemically reacting systems is defined in considerable detail producing highly constrained sets of data for model development.

The experiments described here were conducted in a variable temperature (550 K $< T <$ 1200 K), variable pressure (1 atm $< P <$ 20 atm) flow reactor[52] with residence times ranging from 10 ms to 2 s. The design concept of the variable pressure flow reactor is based on fixing the diagnostic sampling position, and moving the point of fuel injection relative to this location to vary the relative reaction time one wishes to observe. The approach is very similar to that which is normally performed in the study of premixed laminar one-dimensional flames where the burner rather than the diagnostic sampling position is moved. This approach not only permits very short gas sampling residence times to continuous, on-line diagnostic instruments (important for on-line measurement of low-stability molecular species such as aldehydes and other oxygenates), but simple accommodation of optical diagnostics at the sampling location. Crossed-beam optical access ports (normal to the flow direction) are positioned at the same location at which a hot-water-cooled, wall-convection-quenched, gas-sampling probe, and silica-coated thermocouple probe are axially located. Optical diagnostic measurements of OH using existing line resonance absorption or fluorescence techniques[53] and other in situ optical measurements, including in situ Fourier-transform infrared (FTIR), are easily adaptable to the current facility.

A schematic diagram of the variable pressure flow reactor is given in Fig. 7. Nitrogen carrier gas along with the more stable reactants, e.g., H_2 and CH_4, flow from left to right in the figure. The least stable reactants, e.g., N_2O or NO_2, along with about 10% of the total nitrogen carrier flow is injected into the carrier/stable reactant stream at a mixer on the left end of a conical silica foam diffuser. The mixer is jet-stirred and has a nominal turnover time of about 0.5% of the total test time. Various techniques including arc plasmas and electrical resistance have been used to heat the carrier gas upstream of the test section. In the present work, metal oxide deposits on surfaces formed from the deterioration of arc plasma cathodes and anodes, particularly during operation at high pressures, were found to catalytically affect the kinetics of mixtures with oxides of nitrogen. Hence, electric resistance heaters were used in the present work and it is recommended that kinetic studies on mixtures of N_xO_y species should not use arc plasmas as heating sources.

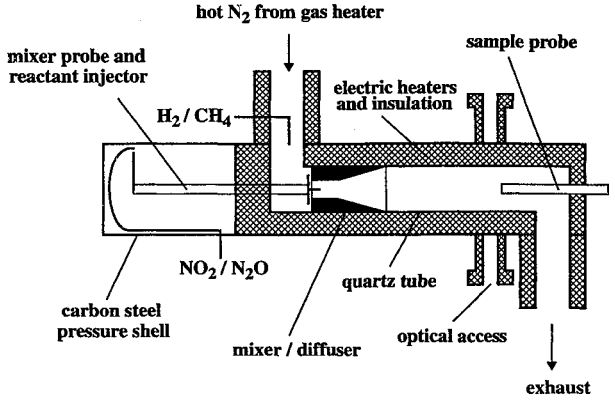

Fig. 7 Schematic diagram of the variable pressure flow reactor.

The shell is made of schedule 12 carbon steel pipe and is ASME code-stamped for operation from full vacuum to 30 atm and 245 to 533 K wall temperature. The pressure shell is designed to enclose not only the reactor section (the reactor duct heaters and insulation), but also the positioning mechanism and reactant injection probe that axially locates the reactant/carrier gas mixing section relative to the sampling position. This design results in very low thrust to move probes (due to pressure drop across flanges) and eliminates the need for critical dynamic seals. Since all flanges are at relatively low temperatures, there is also no need for exotic materials of construction to be used for the pressure shell nor elaborate designs required to maintain pressure seals. The reactor duct itself is a 173-cm-long, 2-mm wall thickness, 10.16-cm i.d., fused silica tube, which extends from a Inconel mating flange at the fuel injection probe entrance to a similar mating flange located at the entrance to the exhaust port of the reactor shell. A maximum distance of about 100 cm is available for collecting kinetic data.

The mixer section is approximately 50 cm long and is machined from a low-porosity, silica foam block to an o.d. about 0.1 mm less than the nominal 10.16-cm i.d. of the cylindrical reactor duct. The interior contour of the mixer section is shaped as a diverging nozzle with a throat diameter of 2.5 cm and an expansion half-angle of 5 deg. The mixer–diffuser section consists of a central round baffle plate that forces the carrier gas flow out to the reactor tube wall and then radially inward through a gap between the plate and the upstream end of the diffuser. Reactant and diluent nitrogen from within the movable probe are then injected in a direction opposite to the carrier gas flow to enable rapid mixing. The reactant injection probe is partially insulated from the carrier flow to prevent premature decomposition/pyrolysis reactions of the nitrogen diluted (unstable) reactant inside the probe. All reactants are premixed into varying amounts of added nitrogen diluent to reduce residence time within the injection probe.

In order to translate flow reactor position into reaction time, the mean velocity distribution along the centerline is measured under cold flow conditions using hot-wire anemometry and pitot-static probes. These measurements are related to experimental conditions through Reynolds number correlations.

A hot-water-cooled, stainless steel sample probe is mounted in the reactor end flange and is used to continuously extract and convectively quench a small portion of the reacting gases. From the probe, the gas sample flow is sent to a FTIR analyzer, a continuous electrochemical analyzer for O_2, continuous nondispersive infra-red (NDIR) analyzers for CO and CO_2, and to a continuous selective thermal conductivity detector for H_2. Data acquired by these instruments are forwarded to an a/d board interface and recorded on a hard-disk-based microprocessor system. A gas sampling and storage technique for interfacing with gas chromatographs and gas chromatograph/mass spectrometers is also available. The sample temperature is measured with a silica coated, fine wire (50 μm diam), Pt/Pt13%Rh thermocouple.

Flow Reactor Model and Sensitivity Analysis

In the case of the steady, isobaric flow reactor, convective transport is large relative to the diffusive transport as a result of operation with high through-put velocities, and thus, the longitudinal gradients are small. This assumption reduces the

steady, one-dimensional conservation equations of mass, species, and energy to the following:

$$M = \rho u A \tag{1}$$

$$M \frac{dY_k}{dx} = A\omega_k W_k \tag{2}$$

$$M \frac{dT}{dx} = -\frac{A}{C_p} \sum_{k=1}^{K} \omega_k h_k W_k \tag{3}$$

In these equations x denotes the independent spatial coordinate; M the mass flow rate; T the temperature; Y_k the mass fraction of the kth species; ρ the mass density; W_k the molecular weight of the kth species; C_p the constant pressure heat capacity of the mixture; h_k the specific enthalpy of the kth species; and A the cross-sectional area of the reactor tube. This model also assumes that reactants are instantaneously mixed at $x = 0$. Although the mixing times are small compared to the overall kinetic times of interest in the flow reactor, the mixing process can affect the kinetics that occur at short distances (small times), e.g., induction periods. Through detailed numerical and experimental studies,[54] we have shown that the uncertainties of the mixing process on the kinetics at small distances are short-lived because of fast underlying radical shuffle reactions. Thus, the assumption of instantaneous mixing of reactants is overcome by choosing a reference position for comparison of model to experiment not at $x = 0$ where the initial conditions are somewhat ill-defined, but at an arbitrary position downstream where the system is well-mixed.

The role of sensitivity analysis is to probe the relationships between the model parameters and the solutions to the governing equations; i.e., the spatial or time-dependent species concentrations, temperature, velocity, etc. In essence, a sensitivity analysis to the above flow reactor model allows questions to be answered concerning 1) interpretation and analysis of models, 2) relationships between model parameters and experiment, and 3) inversion problems. Typical of these questions may be the following:

1) What steps are significant in the mechanism?

2) What role might a particular observation play regarding identification or determination of a particular rate constant?

3) Can alterations in one part of a mechanism be compensated for by changes elsewhere while leaving the observations fixed?

4) Are different observations in the same chemical system truly independent?

5) What physical content resides in identifiable features of concentration or thermal profiles?

6) How can one establish the role of initial species or possibly the effect of the introduction of species during the reaction?

7) By what pathway through the mechanism does one species control the behavior of others?

8) How do the various rate constants work in concert to have major or minor influences on combustion phenomena?

9) Can the role of missing reactions or steps in a mechanism be assessed?

10) How may one quantitatively reduce the number of rate constants or transport coefficients in a reactive system?

11) Can systematic means be found to lump combustion systems?

12) How do statistical errors in the model input propagate to laboratory observations?

13) When inverting laboratory data by residual minimization, what correlations are produced among the data or parameters?

The governing flow reactor equations described in the last section can be generalized as:

$$\boldsymbol{F}(\boldsymbol{O}, \boldsymbol{\alpha}) = 0 \tag{4}$$

where $\boldsymbol{O}$ represents the vector of N dependent variables, and the vector $\boldsymbol{\alpha}$ of length M represents the system parameters such as activation energies, pre-exponential factors, and other quantities that enter the differential equations.

In a sensitivity analysis, the quantities of natural interest are the first-order sensitivity coefficients

$$S_{ij} = \frac{\partial \boldsymbol{O}_i}{\partial \boldsymbol{\alpha}_j} \tag{5}$$

which provide a direct measure of how the jth parameter controls the behavior of the ith dependent variable at point x and time t. The appropriate equations for these quantities can be derived by differentiating Eq. (4) with respect to $\boldsymbol{\alpha}$. Noting that the functional vector $\boldsymbol{F}$ depends on $\boldsymbol{\alpha}$ both explicitly and implicitly through the solution vector $\boldsymbol{O}$, differentiation of Eq. (4) yields

$$\frac{d}{d\boldsymbol{\alpha}_j} \boldsymbol{F}[\boldsymbol{O}(\boldsymbol{\alpha}), \boldsymbol{\alpha}] = \frac{\partial \boldsymbol{F}}{\partial \boldsymbol{O}} \frac{\partial \boldsymbol{O}}{\partial \boldsymbol{\alpha}_j} + \frac{\partial \boldsymbol{F}}{\partial \boldsymbol{\alpha}_j} \tag{6}$$

($j = 1, 2, \ldots, M$). Recalling that the Jacobian matrix is given by $J = \partial \boldsymbol{F}/\partial \boldsymbol{O}$, we have

$$J \frac{\partial \boldsymbol{O}}{\partial \boldsymbol{\alpha}_j} = -\frac{\partial \boldsymbol{F}}{\partial \boldsymbol{\alpha}_j} \tag{7}$$

($j = 1, \ldots, M$). Solution of these equations is generally obtained with the simultaneous solution of the governing equation. Examples of the use of sensitivity analysis are available in the literature.[55-57]

N_2O Decomposition

The elementary unimolecular dissociation of nitrous oxide has been shown to be an important reaction in predicting RDX deflagration.[4] Because N_2O is one of the primary oxidizers produced from RDX, its reactions with simple fuels is important. However, an understanding of the complete thermal decomposition mechanism is necessary prior to studying combinations of fuel and oxidizer systems. In a recent study by Allen et al.,[58] flow reactor experiments were performed over temperature, pressure, and residence time ranges of 1103–1173 K, 1.5–10.5 atm, and 0.2–0.8 s, respectively. Mixtures of approximately 1% N_2O in N_2 were studied with the addition of varying amounts of water vapor, from background to 3580 ppm. Experimentally measured profiles of N_2O, O_2, NO, NO_2, H_2O, and temperature were compared with predictions from detailed kinetic modeling calculations to assess the validity of a reaction mechanism developed from currently available literature thermochemical and rate constant parameters. The results from this study showed significant disagreement in both the overall rates of consumption and the concentrations of secondary products. Over the conditions studied, the rate of nitrous oxide consumption was found to be sensitive to both the elementary dissociation reaction and secondary processes, including some produced by the presence of hydrogenous species, particularly the reaction between N_2O and OH.

Reaction rate constants as a function of pressure for the unimolecular reaction, $N_2O \rightarrow N_2 + O$, were determined by linear least-squares minimization of the modeling predictions with the experimental data. For the secondary reactions, the analysis examined the applicability of recently published rate constant measurements[59] of $N_2O + O \rightarrow NO + NO$ and $N_2O + O \rightarrow N_2 + O_2$ in comparison to previous critically reviewed

rate data.[28,60] The new rate data, which included measurements of N_2O and both NO and O_2, collected at temperatures above 1700 K, further supported a near-unity branching ratio. However, the data also suggested a significantly lower activation energy for the $N_2 + O_2$ product channel than previously recommended. Extrapolation of these results to temperatures relevant to the flow reactor yields a considerably higher total rate for the sum of both channels and contradicts previous branching ratio recommendations near 1000 K.[60,61] Although the mechanistic results from N_2O decomposition alone could not differentiate between which sets of $N_2O + O$ rate constants were more accurate at intermediate temperatures (because the N_2O thermal decomposition reaction was always rate limiting), the combination of the N_2O data with kinetic data collected on CO/N_2O mixtures[62] indicated that for self-consistency between models, the overall rate of $N_2O + O \rightarrow$ products could not be as high as inferred from the Davidson et al.[59] evaluation. Hence, the expressions from Baulch et al.,[60] which are consistent within error limits to the high temperature data of Davidson et al. with regards to branching ratio and rate constants, are currently recommended.

In addition, a newly determined upper limit for the rate constant of the $N_2O + OH \rightarrow HO_2 + N_2$ reaction of 5.66×10^8 cm^3 mol^{-1} s^{-1} at 1123 K was determined in order to achieve agreement between model and experimental NO/NO_2 evolution. This upper limit is considerably less than the rates previously reported in the literature, making this reaction essentially unimportant in nitrous oxide decomposition at the present conditions. Other recent experimental studies on N_2O decomposition[63] and N_2O/H_2 flames[45] have also found a similar reduction in the rate constant as have recent BAC-MP4 and G2 theoretical calculations,[64] the latter yielding an estimated activation energy of 38–40 kcal/mol.

An example of nitrous oxide decomposition at elevated pressure (6 atm) is shown in Fig. 8. In this particular experiment, 25% conversion of the initial N_2O concentration occurred within the residence time of the flow reactor. In addition to the measurement of N_2O consumption, formation of O_2, NO, and NO_2 were observed covering four decades of magnitude in mole fraction. In the figure, the solid lines illustrate the resulting predictions of N_2O disappearance and formation of secondary products after linear least-squares analysis of the unimolecular rate constant of N_2O. Interconversion of NO to NO_2 occurs here primarily through $NO + O + M \rightarrow NO_2 + M$, followed by $NO_2 + O \rightarrow NO + O_2$.

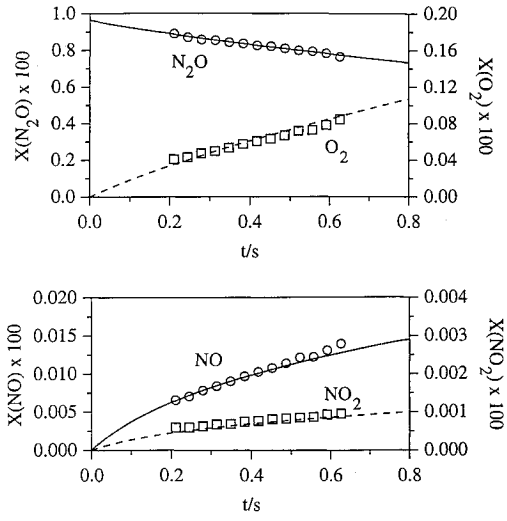

Fig. 8 Species mole fraction profiles for nitrous oxide decomposition at 6 atm and 1123 K. The initial mole fractions of N_2O and H_2O were 9.64×10^{-3} and 5.60×10^{-4}, respectively. Symbols are the experimental data and the lines are the model predictions.

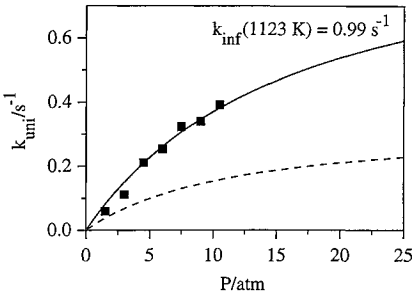

Fig. 9 Pressure dependence of k_{uni} for $N_2O \rightarrow N_2 + O$ at 1123 K. Shown in the figure are the experimental data of Allen et al.[58] at 1123 K, k_{uni} from the review of Tsang and Herron[28] for 700–2500 K, and the recommended rate constant from Ref. 58 with $k_{O,N_2} = 9.13 \times 10^{14} \exp(-57{,}690/RT)$ cm^3 mol^{-1} s^{-1} and $k_\infty = 7.91 \times 10^{10} \exp(-56{,}020/RT)$ s^{-1}.

Hydroxyl radicals produced from hydrogenous species also react with O atoms to produce molecular oxygen and H atoms, the latter species reacting directly with nitrous oxide. The experimentally observed rate was found to be nearly independent of added water concentration.

As shown in Fig. 9, the dissociation reaction is in fall-off over the pressure and temperature ranges studied here. The dashed line in the figure shows the recently recommended[28] fall-off and rate constant expressions to yield significant inconsistencies with the present results. Using literature data for the low pressure limit,[65] and re-evaluating previous high-pressure limit data with the current mechanism, a new expression (solid line) for the unimolecular decomposition of N_2O in N_2 was determined independently, however, in agreement with the present flow reactor results.[58] Note that with the decreased importance of the $N_2O + OH$ reaction, the rate of N_2O unimolecular decomposition and its pressure dependence in nitramine decomposition are even more important. These studies have also illustrated a situation in the hierarchical construction of reaction mechanisms where an originally assumed simpler kinetic system (N_2O decomposition) had to be refined after studying a more complex mixture ($CO/H_2O/N_2O$).

H_2/NO_2 Reaction

Just as previously described for nitrous oxide, flow reactor studies have also been conducted on the thermal decomposition of nitrogen–dioxide.[66] These studies have confirmed the importance of the bimolecular self-reaction of NO_2 at flow reactor temperatures. The next more complicated system in the hierarchical development of these chemical systems is the H_2/NO_2 (and N_2O) reactions. Yetter et al.[67] have reported on flow reactor studies of this system over the temperature range of 694–944 K and pressure range of 1–12 atm. Model predictions for the profiles of H_2O, NO_2, NO, and temperature were compared with the corresponding experimentally measured profiles. The predicted overall reaction rate was observed to be approximately 2–3 times too fast based on literature rate constant parameters. Reaction flux and sensitivity analyses identified the reactions

$$H_2 + OH \rightarrow H_2O + H$$

$$H_2 + NO_2 \rightarrow H + HONO$$

$$HONO + OH \rightarrow H_2O + NO_2$$

$$NO_2 + H \rightarrow NO + OH$$

$$NO + OH + M \rightarrow HONO + M$$

$$HNO + NO_2 \rightarrow HONO + NO$$

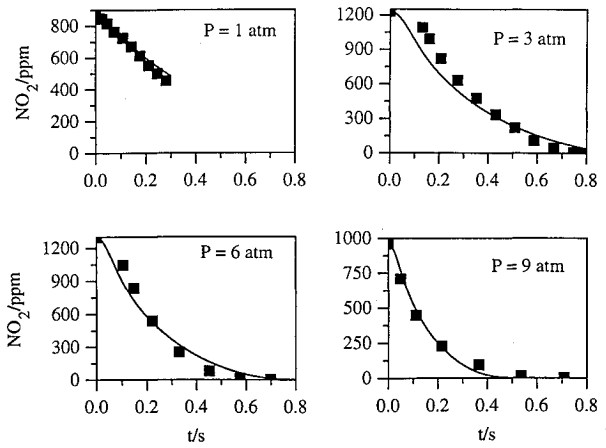

Fig. 10 Experimental and modeling mole fraction profiles for the reaction of H_2 [$X_i(H_2)$ = 5700 ppm] and NO_2 at 833 K for pressures of 1 atm [$X_i(NO_2)$ = 860 ppm], 3 atm [$X_i(NO_2)$ = 1230 ppm], 6 atm [$X_i(NO_2)$ = 1300 ppm] and 9 atm [$X_i(NO_2)$ = 960 ppm].

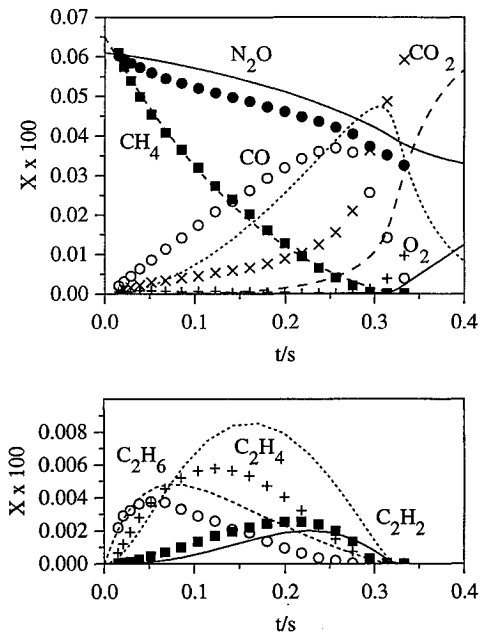

Fig. 11 Species mole fraction profiles for a $CH_4/N_2O/N_2$ mixture reacting at 3.3 atm and 1153 K. Symbols are the experimental data and lines the corresponding model predictions. The N_2O mole fraction has been divided by a factor of 10.

as the most important (listed in decreasing order of importance). Among these reactions, the rate constant of $H_2 + NO_2 \rightarrow HONO + H$ had the largest uncertainty. There are currently no direct rate constant measurements for this reaction. With adjustments of this rate constant within its uncertainty limits (factor of 4 decrease below the value recommended in Ref. 28), good agreement between model and experiment was obtained. Examples of the results are shown in Fig. 10 for four pressures (1, 3, 6 and 9 atm). A pressure dependency of $P^{0.5}$ was determined for the rate of the overall reaction.

CH_4/N_2O Reaction

Further up the hierarchical ladder in complexity are the kinetics of CH_4 and N_2O (and NO_2) mixtures. An example of flow reactor studies on the CH_4/N_2O system has been reported by Allen et al.,[68] which covers the temperature, pressure, and residence time ranges of 1120–1173 K, 3.3 atm, and 300–450 ms, respectively. Equivalence ratios were varied from 0.24 to 1.0 at a constant mole fraction of N_2O in nitrogen. Experimentally measured profiles of CH_4, C_2H_6, C_2H_4, C_2H_2, CO_2, CO, O_2, H_2O, N_2O, NO, and temperature were compared with model predictions. This model used the same basis set of thermochemical and kinetic parameters as those described for the submodels shown previously plus reactions validated from CO and CH_2O submodels. A comparison between model prediction and experiment (Fig. 11) shows good agreement. Some discrepancies are still observed among the minor hydrocarbon species and the formation of CO and CO_2.

The three examples above are typical of submodel validation and by themselves provide important information on the reaction dynamics over limited temperature, pressure, and concentration ranges. Development of the desired comprehensive gas-phase reaction mechanisms is not complete until the models have been tested against data obtained from all other validation experiments as previously mentioned. As these validation experiments are completed, models for RDX combustion may be iteratively refined.

RDX Model Development and Analysis

A model for RDX gas-phase combustion has been developed starting with the RDX decomposition mechanism of Melius[4] and adding to this mechanism the species and reactions reviewed by Tsang and Herron[28] and Tsang[69] from their proposed reaction grid. This chemistry has been further modified to adopt the $H_2/CO/O_2$ chemical submodel of Kim et al.[70] Finally, further refinements have been made to this model from recent flow reactor studies, such as those described previously, shock-tube studies, static reactor studies, and flame studies. With this model, Fetherolf and Litzinger[13] have had relatively good success in predicting gas-phase species profiles above deflagrating RDX.

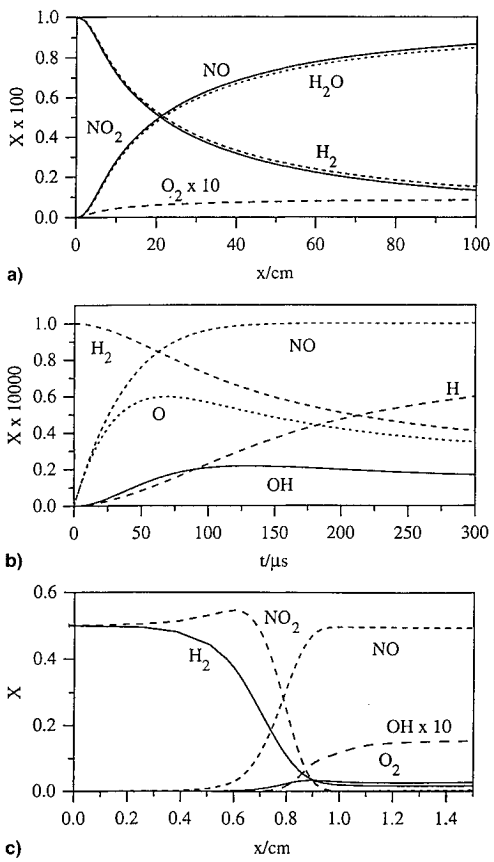

Fig. 12 Simulated experiments with H_2/NO_2 mixtures: a) flow reactor [$X_i(H_2)$ = 0.01, $X_i(NO_2)$ = 0.01, balance N_2, T_i = 960 K, P = 1 atm]; b) shock tube [$X_i(H_2)$ = 100 ppm, $X_i(NO_2)$ = 100 ppm, balance Ar, T_i = 2200 K, P = 1 atm]; and c) premixed flame [$X_i(H_2)$ = 0.5, $X_i(NO_2)$ = 0.5, T_i = 298 K, P = 0.1 atm].

Table 1 Reactions with high sensitivity in H_2/NO_2 mixtures

Flow reactor	Shock tube	Premixed flame
$H_2 + OH = H_2O + H$	$O + H_2 = H + OH$	$OH + H_2 = H_2O + H$
$H_2 + NO_2 = HONO + H$	$NO_2 + O = NO + O_2$	$NO + O(+M) = NO_2(+M)$
$HONO + OH = NO_2 + H_2O$	$OH + H_2 = H_2O + H$	$O + H_2O = OH + OH$
$HO_2 + HO_2 = H_2O_2 + O_2$	$NO + O(+M) = NO_2(+M)$	$NO_2 + O = NO + O_2$
$HO_2 + OH = H_2O + O_2$	$H + O_2 = O + OH$	$H + O_2 = O + OH$
$OH + NO(+M) = HONO(+M)$	$NO_2 + H = NO + OH$	$NO_2 + NO_2 = 2NO + O_2$
$O + H_2O = OH + OH$	$O + H_2O = OH + OH$	$O + H_2 = H + OH$
$NO_2 + NO_2 = 2NO + O_2$	$NO_2 + OH = NO + HO_2$	$NO + H = N + OH$
$NO_2 + H = NO + OH$	—	$HO_2 + OH = H_2O + O_2$
$NO_2 + OH = NO + HO_2$	—	$NO + OH(+M) = HONO(+M)$
$H_2O_2(+M) = OH + OH(+M)$	—	$NO_2 + H = NO + OH$
$NO + H(+M) = HNO(+M)$	—	$H_2 + NO_2 = HONO + H$

Table 2 Reactions with high sensitivity in HCN/NO_2 mixtures

Flow reactor	Shock tube	Premixed flame
$T_i = 1200$ K, $P = 6$ atm $X_i(HCN) = 2 \times 10^{-3}$, $X_i(NO_2) = 1 \times 10^{-3}$, balance N_2	$T_i = 2200$ K, $P = 1$ atm $X_i(HCN) = 2 \times 10^{-4}$, $X_i(NO_2) = 1 \times 10^{-4}$, balance Ar	$T_i = 298$ K, $P = 0.1$ atm $X_i(HCN) = 0.66$, $X_i(NO_2) = 0.34$
$HCN + O = CN + OH$	$HCN + O = NCO + H$	$N_2O(+M) = N_2 + O(+M)$
$NO_2 + O = NO + O_2$	$HCN + O = CN + OH$	$HCN + O = NCO + H$
$CN + NO_2 = NCO + NO$	$CN + OH = NCO + H$	$NCO(+M) = N + CO(+M)$
$NO_2 + NO_2 = 2NO + O_2$	$N + NO = N_2 + O$	$N + NO = N_2 + O$
$NCO + O = CN + O_2$	$NO + H = N + OH$	$NO + O(+M) = NO_2(+M)$
$NCO + NO = CO + N_2 + O$	$NH + O = NO + H$	$NCO + NO = N_2O + CO$
$CN + HCN = C_2N_2 + H$	$CN + O = CO + N$	$CO + OH = CO_2 + H$
$HCN + O = NH + CO$	$CN + H_2 = H + HCN$	$H + OH + M = H_2O + M$
$NCO + NO = CO_2 + N_2$	$NCO(+M) = N + CO(+M)$	$NCO + NO_2 = CO + 2NO$
$NCO + NO = N_2O + CO$	$HCN + O = NH + CO$	$NH + OH = HNO + H$
$NCO + NO_2 = CO + 2NO$	$H + O_2 = OH + O$	$NCO + O = CN + O_2$
$NO + O(+M) = NO_2(+M)$	$NO_2 + O = NO + O_2$	$CN + OH = NCO + H$
$NCO + NO_2 = CO_2 + N_2O$	$NO_2 + H = NO + OH$	$HCN(+M) = H + CN(+M)$
$CO + OH = CO_2 + H$	$NCO + NO_2 = CO + 2NO$	$NO + H = N + OH$
$HNCO + OH = H_2O + NCO$	$NH + NO = N_2O + H$	$NH + NO = N_2O + H$
$NH + NO = N_2 + OH$	—	$NH_2 + NO = NNH + OH$
$HCN + OH = HOCN + H$	—	$NCO + H = NH + CO$
$CN + H_2O = HCN + OH$	—	$HNCO + H = NH_2 + CO$
$T_i = 1200$ K, $P = 6$ atm $X_i(HCN) = 2 \times 10^{-3}$, $X_i(N_2O) = 1 \times 10^{-3}$, $X_i(NO) = 1 \times 10^{-3}$, balance N_2	$T_i = 2200$ K, $P = 1$ atm $X_i(HCN) = 1 \times 10^{-3}$, $X_i(N_2O) = 5 \times 10^{-4}$, $X_i(NO) = 5 \times 10^{-4}$, balance Ar	
$N_2O(+M) = N_2 + O(+M)$	$NCO + O = CO + NO$	—
$N_2O + H = N_2 + OH$	$NCO + H = NH + CO$	—
$HNO + OH = H_2O + NO$	$N_2O + H = N_2 + OH$	—
$HOCN + H = HNCO + H$	$NH + O = N + OH$	—
$C_2N_2 + OH = HOCN + CN$	$CO + OH = CO_2 + H$	—
$C_2N_2 + O = NCO + CN$	$N + H_2 = H + NH$	—
$NO_2 + H = NO + OH$	$NH + NO = N_2 + OH$	—
$HCN + OH = H + HCNO$	$NCO + NO = CO_2 + N_2$	—
—	$CN + H_2O = OH + HCN$	—

To numerically illustrate the hierarchical methods of model construction for both chemical systems and experimental techniques, a number of computer simulations of flow reactor, shock-tube, and premixed flame experiments for H_2/NO_2 and HCN/NO_2 mixtures have been conducted using the RDX mechanism described. Sensitivity analysis is applied to identify the most sensitive reactions in each chemical and experimental system. These results are then compared to the reactions that the deflagration velocity of RDX is most sensitive.[4] Finally, homogeneous ignition characteristics of RDX are reported and the dominant reaction pathways of the present mechanism are compared to those reported earlier by Melius.[4,16]

Numerical results simulating the kinetics in a flow reactor experiment, a shock-tube experiment, and a premixed flame are shown in Fig. 12 for an equal molar mixture of H_2 and

NO_2. The model predictions illustrate the time and spatial scales of each experiment and typical species that could be measured experimentally. The results of a sensitivity analysis for the three experiments are presented in Table 1. Note that the combination of reactions important to the shock tube and flow reactor are the same as those important to the flame. However, for the flame, diffusivities of radicals and energy (although not listed in Table 1) can be equally important parameters in the model, and hence, model validation in the flame includes both transport and chemistry.[71] The underlined reactions in Table 1 indicate the well-studied H_2/O_2 reactions. The other reactions are from the NO_x formation and destruction mechanism, some of which have rate constants that are not as well known.

In Table 2, sensitivity analysis results are presented for an HCN/NO_2 mixture, which were obtained from a similar series

Table 3 Chemical reactions governing RDX burn rate

$N_2O(+M) = N_2 + O(+M)$
$N + OH = NO + H$
$N + NO = N_2 + O$
$H_2CN + M = HCN + H + M$
$H_2CN + NO_2 = H_2CNO + NO$
$H_2CN + NO = HCN + HNO$
$RDXRO(+M) \rightarrow 2H_2CNNO_2 + H_2CN(+M)$
$CN + OH = NCO + H$
$HNO + OH = NO + H_2O$
$NH + OH = HNO + H$
$H + OH + M = H_2O + M$
$NH_2 + NO = NNH + OH$
$H_2CN + NO_2 = HCN + HONO$

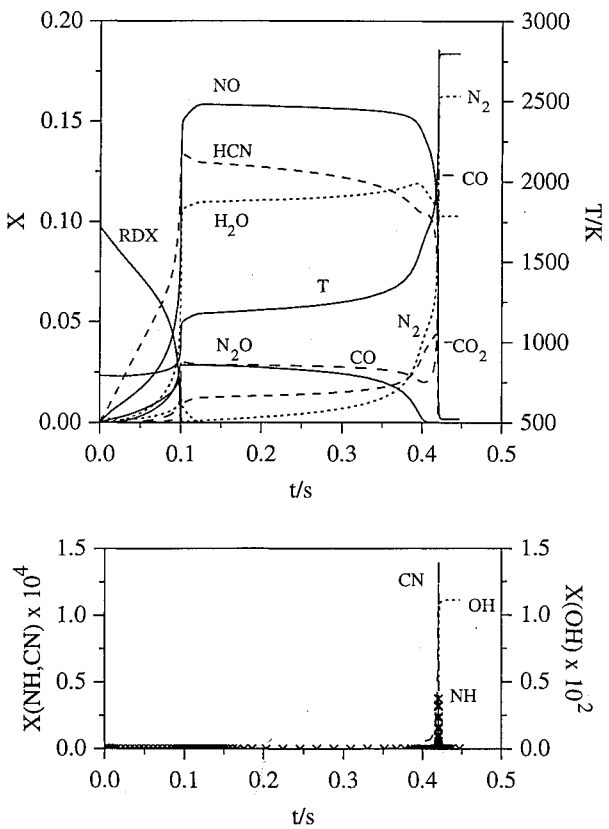

Fig. 13 Temperature and species mole fraction profiles for RDX ignition at 1 atm and 800 K. The initial mixture composition consisted of 0.10 RDX and the balance Ar.

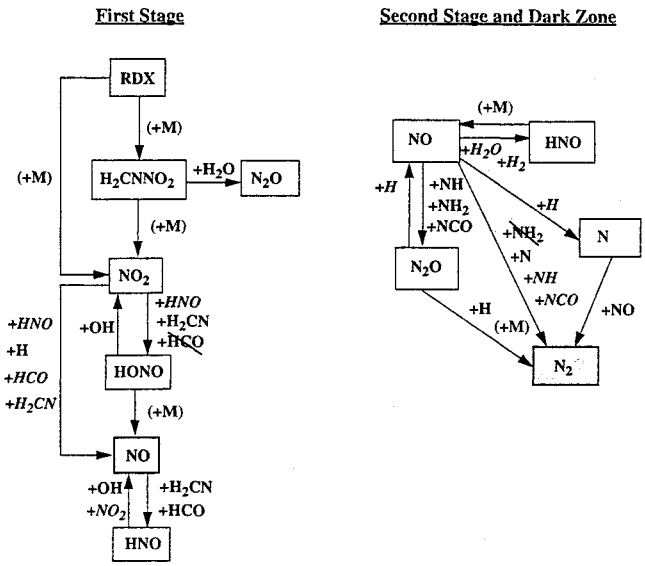

Fig. 14 RDX ignition: the nitrogen chemistry of the NO_2 group. The italic species indicate a change in the reaction pathways of the revised mechanism. Species that are crossed-out indicate reaction pathways that are of less importance.

of flow reactor, shock-tube, and premixed flame calculations. The underlined reactions include all the reactions that were important in the H_2/NO_2 studies. Note again that the reactions important for the flame are the same as those important for the combined shock-tube and flow reactor studies. Also note that the total number of important reactions to both HCN/NO_2 and H_2/NO_2 mixtures is small compared to the total number of possible kinetic interactions as described in the reaction grid of Tsang and Herron (approximately 350 steps). At the bottom of Table 2, reactions found important in an $HCN/N_2O/NO$ mixture and not found sensitive in the HCN/NO_2 mixture are listed. These differences illustrate how different subsets of reactions are emphasized for the different oxidizer systems. For a particular chemical system, the equivalence ratio, pressure, and temperature also affect which reactions are most sensitive.

Table 3 presents the reactions that govern the RDX burn rate.[4] The underlined reactions include all steps found to be important in the HCN/NO_2 and H_2/NO_2 mixtures. Note that the only reactions of importance to the RDX burn rate not studied in these mixtures are the initial decomposition reactions of RDX and its secondary fragments. The results of Tables 1–3 emphasize the importance of systematic construction of reaction mechanisms and the importance of mechanism development via kinetic data from different types of experiments. These results also suggest that a simple nitramine be added to the hierarchical list of chemical systems (Fig. 6) for gas-phase kinetics model validation.

In Fig. 13, predictions of species and temperature profiles during the homogeneous ignition of RDX are reported for a mixture initially composed of 10% by volume RDX with the remainder of the mixture Ar. The initial temperature and pressure were 800 K and 1 atm, respectively. The species and temperature profiles depict the characteristic two-zone structure. The temperature at the end of the first stage of ignition is approximately 1250 K. At 0.1 s, the composition consists of

$$RDX \rightarrow 0.18H_2O + 0.27NO + 0.07N_2O + 0.03NO_2$$
$$+0.04CO + 0.01CO_2 + 0.34HCN + 0.04CH_2O$$
$$+ 0.01H_2$$

Due to the rapid consumption of CH_2O and NO_2, the composition quickly changes to (at t = 0.11 s)

$$\text{RDX} \rightarrow 0.23H_2O + 0.005N_2 + 0.33NO + 0.06N_2O + 0.01NO_2 + 0.06CO + 0.02CO_2 + 0.28HCN + 0.005HNCO$$

The trends of these results are in relatively good agreement with the RDX deflagration results of Korobeinichev et al.[7] However, N_2 is significantly underpredicted in the present model in comparison to both the results of Korobeinichev et al.[7] and Fetherolf and Litzinger.[13] In the present model, small quantities of N_2 are formed during the first stage mainly through reaction of NCO with NO and through reaction of N_2O with H-atoms. The NO from the first stage may be assumed to be produced almost entirely from NO_2 and the CO and CO_2 from CH_2O. Summing the N_2O + N_2 yield and comparing this mole fraction with the sum of the CH_2O + CO + CO_2 yield shows nearly the same values in the model predictions and in the experimental results. This result is not surprising since it represents the overall channel of RDX → $3CH_2O$ + $3N_2O$. Similar results are also obtained if the HCN mole fractions are compared to the sum of the NO and NO_2 mole fractions. From these sums, the overall branching ratios of RDX decomposition may be deduced from the experiments and model. For the model, approximately 22% of the RDX is found to yield CH_2O + N_2O at 1250 K. A yield of 30% is obtained at 1308 K from the experimental results of Korobeinichev et al.[7] and a yield of 50% at 936 K from the results of Fetherolf and

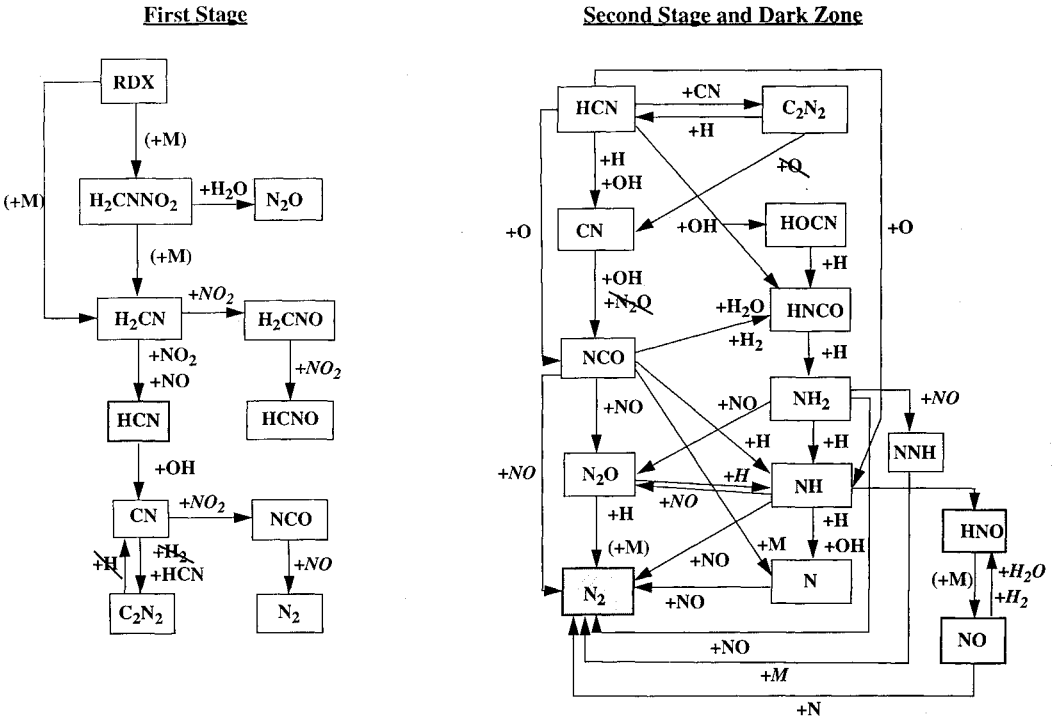

Fig. 15 RDX ignition: the amino nitrogen chemistry.

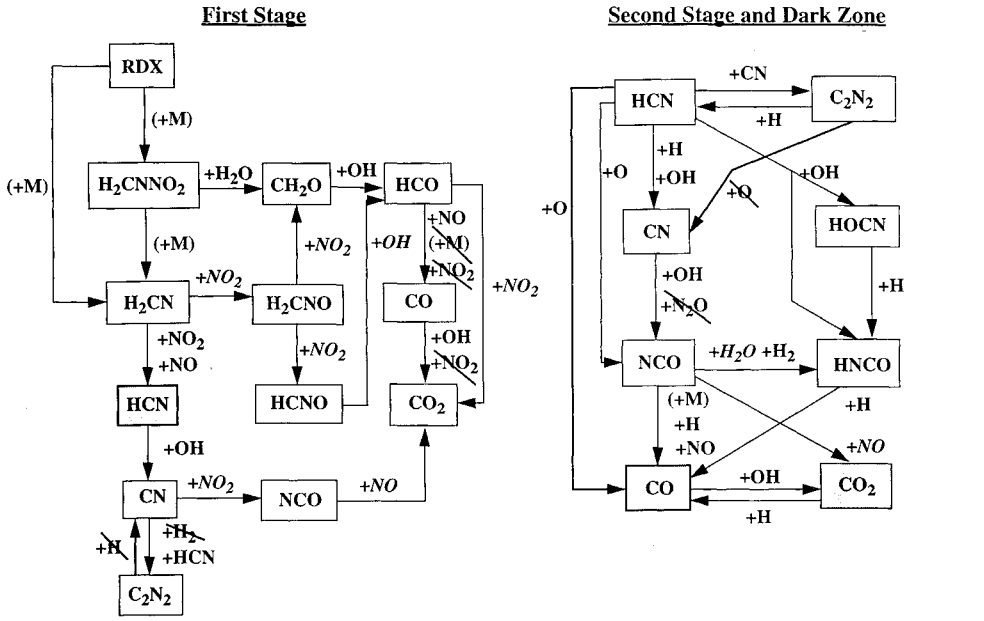

Fig. 16 RDX ignition: the carbon chemistry.

Table 4 Reactions with high sensitivity in RDX ignition

First-stage reaction	Second-stage reaction and dark zone
$RDXRO(+M) \rightarrow 2H_2CNNO_2 + H_2CN(+M)$	$N_2O(+M) = N_2 + O(+M)$
$H_2CNNO_2(+M) = H_2CN + NO_2(+M)$	$N_2O + H = N_2 + OH$
$H_2CNNO_2 + H_2O = CH_2O + N_2O + H_2O$	$HNO + OH = H_2O + NO$
$H_2CN + NO_2 = H_2CNO + NO$	$HNO + NO = N_2O + OH$
$H_2CN + NO_2 = HCN + HONO$	$NO + H_2 = HNO + H$
$H_2CN + NO = HCN + HNO$	$CO + OH = CO_2 + H$
$H_2CNO + NO_2 = CH_2O + 2NO$	$HCN + OH = H + HOCN$
$H_2CNO + NO_2 = HCNO + HONO$	$HNCO + H = NH_2 + CO$
$CH_2O + OH = HCO + H_2O$	$HOCN + H = HNCO + H$
$HONO + OH = H_2O + NO_2$	$HNCO + CN = HCN + NCO$
$NO + OH(+M) = HONO(+M)$	$NCO + NO = CO + N_2 + O$
$NO_2 + HCO = H + CO_2 + NO$	$NCO + NO = CO_2 + N_2$
$NO_2 + H = NO + OH$	$NH_2 + NO = NNH + OH$
$NO_2 + H_2 = HONO + H$	$NH_2 + NO = N_2 + H_2O$

Litzinger.[13] A maximum yield of about 16% is suggested from the isolated molecule experiments of Zhao et al.[19] These results show, as has been reported previously in the literature, the change in branching ratio of RDX decomposition with temperature. Consistent with the agreement in speciation and temperature of the post primary zone as noted above, the branching ratio trends of the model are closest to the experimental results of Korobeinichev et al.[7] In comparison to the experimental results of Hanson-Parr and Parr,[14,15] who report nonintrusive data close to the burning surface, the maximum amounts of NO_2 formed relative to NO appear to be too small in the model predictions. Furthermore, the NO_2 that is formed in the model appears to be consumed too fast relative to the consumption of N_2O. However, the formation and consumption of CN and NH, and the formation of OH, during ignition of the second stage are consistent with the observations of Hanson-Parr and Parr.[14,15]

Reaction pathways for the chemistry of the nitrogen atoms in the nitro group, the chemistry of the nitrogen atoms of the amino group, and the chemistry of the carbon atoms are shown in Figs. 14, 15, and 16, respectively. These figures were originally derived by Melius and have been updated here with results from the current mechanism. The italic species names indicate new channels of importance. The species names that are crossed-out are no longer of significance. Compared to the original model of Melius,[16] and even to the more recent model,[4] the present model update, achieved through submodel validation, has affected the pathways of many species. For example, during the first stage, HNO in the present model plays a more significant role in the conversion of NO_2 to HONO and NO, whereas HCO plays a much lesser role. Also, the formation of N_2 in the first stage results from reactions of NCO with NO and N_2O with H-atoms and not from reaction of N_2O with CO or OH as might be inferred from the review of Tsang and Herron.[28] Because the rate constant for the reaction of N_2O with H-atoms is well-established, significant changes would have to occur in other steps of the model to produce the yields of N_2 measured experimentally. Furthermore, it is interesting to note that no condensed-phase models for RDX suggest a route for N_2 formation. Finally, Table 4 gives the most sensitive (rate-controlling) reactions on the major species during RDX ignition. Again, these reactions are consistent with those found important to the burning rate (Table 3).

Summary

The present work has demonstrated the application of hierarchical model construction through the application of different experimental techniques and different chemical systems. From the results of validation experiments of chemical submodels, the RDX decomposition model of Melius has been updated. Although the general trends of the two models are consistent, differences are observed in many of the pathways of secondary reactants. The model is currently being updated with the inclusion of the HNC isomer of HCN and its reaction chemistry.[72] Validation data are presently needed on simple nitramines to further refine the chemistry during the first stage of reaction. The present work has reported on fundamental kinetic experiments with only a modest variation in pressure above atmospheric. Although literature rate data were found to generally predict the trends of the experiments, the model required refinement to accurately predict the data. Theories and numerical codes are presently available to investigate large excursions above atmospheric pressure.[73,74] However, kinetic data on all the chemical systems described in this article (as well as on specific reactions and equations of state) will be needed to confirm and validate the submodels.

Acknowledgments

The authors wish to acknowledge support from the Office of Naval Research, under Contract N00014-90-J-4062, and to acknowledge R. S. Miller as Technical Monitor. The authors also acknowledge Carl Melius of Sandia National Laboratories for the transfer of his RDX mechanism and helpful technical discussions.

References

[1]Alexander, M. H., Dagdigian, P. J., Jacox, M. E., Kolb, C. E., Melius, C. F., Rabitz, H., Smooke, M. D., and Tsang, W., "Nitramine Propellant Ignition and Combustion Research," *Progress in Energy and Combustion Science*, Vol. 17, No. 4, 1991, pp. 263–296.

[2]Yetter, R. A., and Dryer, F. L., "Experimental, Modeling, and Sensitivity Analysis Studies of Gas-Phase Reaction Mechanisms Important to the Combustion of High Energy Density Materials," Annual Rept., Office of Naval Research, Contract N00014-90-J-4062, Arlington, VA, Sept. 1990.

[3]Yetter, R. A., Dryer, F. L., Allen, M. T., and Ilincic, N., "Kinetic Studies on Gas-Phase Reaction Mechanisms Important to the Combustion Process of High Energy Density Materials," 28th JANNAF Combustion Meeting, San Antonio, TX, Nov. 1991.

[4]Melius, C. F., "Thermochemical Modeling: II. Application to Ignition and Combustion of Energetic Materials," *Chemistry and Physics of Energetic Materials*, edited by S. N. Bulusu, Kluwer Academic, The Netherlands, 1990, pp. 51–78.

[5]Westbrook, C. K., and Dryer, F. L., "Chemical Kinetic Modeling of Hydrocarbon Combustion," *Progress in Energy and Combustion Science*, Vol. 10, No. 1, 1984, pp. 1–57.

[6]Perrini, A., Yetter, R. A., and Dryer, F. L., "On the Development of Comprehensive Reaction Mechanisms," *Combustion Science and Technology* (submitted for publication).

[7]Korobeinichev, O. P., Kuibida, L. V., Orlov, V. N., Tereschenko, A. G., Kutsenogii, K. P., Mavliev, R. A., Ermolin, N. E., Fomin, V. M., and Emel'yanov, I. D., "Mass Spectrometric Probe Study of the Flame Structure and Kinetics of Chemical Reactions in Flames," *Mass-Spektrometriya i Khimicheskaya Kinetika*, 1985, pp. 73–93.

[8]Ermolin, N. E., Korobeinichev, O. P., Kuibida, L. V., and Fomin, V. M., "Study of the Kinetics and Mechanism of Chemical Reactions in Hexogen Flames," *Fizika Goreniya i Vzryva*, Vol. 22, No. 5, 1986, pp. 54–64; Translation in *Combustion, Explosion, and Shock Waves*, Vol. 22, No. 5, 1986, pp. 544–553.

[9]Ermolin, N. E., Korobeinichev, O. P., Kuibida, L. V., and Fomin, V. M., "Processes in Hexogene Flames," *Fizika Goreniya i Vzryva*, Vol. 24, No. 4, 1988, pp. 21–29; Translation in *Combustion, Explosion, and Shock Waves*, Vol. 24, No. 4, 1988, pp. 400–407.

[10]Cosgrove, J. D., and Owen, A. J., "The Thermal Decomposition of 1,3,5 Trinitro Hexahydro 1,3,5 Triazine (RDX) Part I: the Products and Physical Parameters," *Combustion and Flame*, Vol. 22, No. 1, 1974, pp. 13–18.

[11]Cosgrove, J. D., and Owen, A. J., "The Thermal Decomposition of 1,3,5 Trinitro Hexahydro 1,3,5 Triazine (RDX) Part II: The Effects of the Products," *Combustion and Flame*, Vol. 22, No. 1, 1974, pp. 19–22.

[12]Benreuven, M., Caveny, L. H., Vichnevetsky, R., and Summerfield, M., "Flame Zone and Subsurface Reaction Model for Deflagrating RDX," *16th Symposium (International) on Combustion*, The Combustion Inst., Pittsburgh, PA, 1976, pp. 1223–1233; also *AIAA Journal*, Vol. 19, No. 10, 1981, pp. 1276–1285.

[13]Fetherolf, B. L., and Litzinger, T. A., "Chemical Structure of the Gas-Phase Above Deflagrating RDX: Comparison of Experimental Measurements and Model Predictions," 30th JANNAF Combustion Subcommittee Meeting, Monterey, CA, Nov. 1993.

[14]Hanson-Parr, D., and Parr, T., "RDX Flame Structure and Chemistry," 30th JANNAF Combustion Subcommittee Meeting, Monterey, CA, Nov. 1993.

[15]Hanson-Parr, D., and Parr, T., "RDX Flame Structure," 25th Symposium (International) on Combustion, The Combustion Inst., Pittsburgh, PA, 1994, pp. 1635–1643.

[16]Melius, C. F., "Theoretical Studies of the Chemical Reactions Involved in the Ignition of Nitramines," 24th JANNAF Combustion Subcommittee Meeting, Monterey, CA, Oct. 1987.

[17]Melius, C. F., "Thermochemical Modeling: I. Application to Decomposition of Energetic Materials," *Chemistry and Physics of Energetic Materials*, edited by S. N. Bulusu, Kluwer Academic, The Netherlands, 1990, pp. 21–49.

[18]Shaw, R., and Walker, F. E., "Estimated Kinetics and Thermochemistry of Some Initial Unimolecular Reactions in the Thermal Decomposition of 1,3,5,7-Tetranitro-1,3,5,7-tetraazacyclooctane in the Gas Phase," *Journal of Physical Chemistry*, Vol. 81, No. 25, 1977, pp. 2572–2576.

[19]Zhao, X., Hintsa, E. J., and Lee, Y. T., "Infrared Multiphoton Dissociation of RDX in a Molecular Beam," *Journal of Chemical Physics*, Vol. 88, No. 2, 1988, pp. 801–810.

[20]Li, S. C., and Williams, F. A., "Nitramine Deflagration: A Reduced Chemical Mechanism for the Primary Flame," AIAA Paper 94-3041, June 1994.

[21]Oyumi, Y., and Brill, T. B., "Thermal Decomposition of Energetic Materials 3. A High-Rate, In-Situ, FTIR Study of the Thermolysis of RDX and HMX with Pressure and Heating Rate as Variables," *Combustion and Flame*, Vol. 62, No. 3, 1985, pp. 213–224.

[22]Brill, T. B., Brush, P. J., Patil, D. G., and Chen, J. K., "Chemical Pathways at the Burning Surface," 24th Symposium (International) on Combustion, The Combustion Inst., Pittsburgh, PA, 1992, pp. 1907–1914.

[23]Brill, T. B., and Brush, P. J., "Condensed Phase Chemistry of Explosives and Propellants at High Temperature: HMX, RDX, and BAMO," *Philosophical Transactions of the Royal Society of London, Series A: Mathematics and Physical Sciences*, Vol. 339, No. 1654, 1992, pp. 377–385.

[24]Brill, T. B., "Connecting the Chemical Composition of a Material to its Combustion Characteristics," *Progress in Energy and Combustion Science*, Vol. 18, No. 2, 1992, pp. 91–116.

[25]Behrens, R., Jr., and Bulusu, S., "Thermal Decomposition of Energetic Materials 3. Temporal Behaviors of the Rates of Formation of the Gaseous Pyrolysis Products of Condensed Phase Decomposition of 1,3,5-Trinitrohexahydro-s-Triazine," *Journal of Physical Chemistry*, Vol. 96, No. 22, 1992, pp. 8877–8891.

[26]Behrens, R., Jr., and Bulusu, S., "Thermal Decomposition of Energetic Materials 4. Deuteriom Isotope Effects and Isotopic Scrambling (H/D, $^{13}C/^{18}O$, $^{14}N/^{15}N$) in Condensed-Phase Decomposition of 1,3,5-Trinitrohexahydro-s-Triazine," *Journal of Physical Chemistry*, Vol. 96, No. 22, 1992, pp. 8891–8897.

[27]Behrens, R., Jr., Land, T. A., and Bulusu, S., "Thermal Decomposition Mechanisms of 1-Nitroso-3,5-Dinitro-s-Triazine (OND-NTA)," 30th JANNAF Combustion Subcommittee Meeting, Monterey, CA, Nov. 1993.

[28]Tsang, W., and Herron, J. T., "Chemical Kinetic Data Base for Propellant Combustion: I Reactions Involving NO, NO_2, HNO, HONO, HCN, and N_2O," *Journal of Physical Chemistry, Reference Data*, Vol. 20, No. 4, 1991, pp. 609–664.

[29]Fetherolf, B. L., and Litzinger, T. A., "Physical and Chemical Processes Governing the CO2 Laser-Induced Deflagration of Ammonium Dinitramide (ADN)," 29th JANNAF Combustion Subcommittee Meeting, Hampton, VA, Nov. 1992.

[30]Brill, T. B., Brush, P. J., and Patil, D. G., "Thermal Decomposition of Energetic Materials 5. Chemistry of Ammonium Nitrate and Ammonium Dinitramide near the Burning Surface Temperature," *Combustion and Flame* (to be published).

[31]Fifer, R. A., "High Temperature Pyrolysis of Methyl (and Ethyl) Nitrate," 17th Symposium (International) on Combustion, The Combustion Inst., Pittsburgh, PA, 1979, pp. 587–599.

[32]Yetter, R. A., and Rabitz, H., "Modeling and Sensitivity Analysis of Nitrate Esters Thermal Decomposition," Geo-Centers, Inc., Report GC-1686-89-014, U.S. Army, Dec. 1989.

[33]Lin, C.-Y., Wang, H.-T., Lin, M. C., and Melius, C. F., "A Shock Tube Study of the $CH_2O + NO_2$ Reaction at High Temperatures," *International Journal of Chemical Kinetics*, Vol. 22, No. 5, 1990, pp. 452–482.

[34]He, Y., Lin, M. C., Wu, C. H., and Melius, C., "The Reaction of HNCO with NO_2 in Shock Waves," *24th Symposium (International) on Combustion*, The Combustion Inst., Pittsburgh, PA, 1992, pp. 711–717.

[35]He, Y., and Lin, M. C., "Effects of Nitric Oxide on the Thermal Decomposition of Methyl Nitrite: Overall Kinetics and Rate Constants for HNO + HNO and HNO + 2NO Reactions," *International Journal of Chemical Kinetics*, Vol. 24, No. 8, 1992, pp. 743–760.

[36]He, Y., Liu, X., Lin, M. C., and Melius, C. F., "Thermal Reaction of HNCO with NO_2 at Moderate Temperatures," *International Journal of Chemical Kinetics*, Vol. 25, No. 10, 1993, pp. 845–863.

[37]He, Y., Lin, M. C., and Melius, C. F., "Theoretical Aspects of the H/N/O-Chemistry Relevant to the Thermal Reduction of NO by H_2," *Progress in Energy and Combustion Science* (submitted for publication).

[38]Fifer, R. A., and Holmes, H. E., "Kinetics of the HCN + NO_2 Reaction behind Shock Waves," *Journal of Physical Chemistry*, Vol. 86, No. 15, 1982, pp. 2935–2944.

[39]Wu, C. H., Wang, H.-T., Lin, M. C., and Fifer, R. A., "Kinetics of CO and H Atom Production from the Decomposition of HNCO in Shock Waves," *Journal of Physical Chemistry*, Vol. 94, No. 8, 1990, pp. 3344–3347.

[40]Mertens, J. D., Chang, A. Y., Hanson, R. K., and Bowman, C. T., "A Shock Tube Study of NH with NO, O_2, and O," *International Journal of Chemical Kinetics*, Vol. 23, No. 2, 1991, pp. 173–196.

[41]Volponi, J. V., and Branch, M. C., "Flame Structure of H_2-NO_2-Argon Laminar Premixed Flames," Western States Section of the Combustion Inst., Paper WSS/CI 90-02, Oct. 1990.

[42]Branch, M. C., Sadeqi, M. E., Alfaragedhi, A. A., and Van Tiggelan, P. J., "Measurements of the Structure of Laminar Pre-Mixed Flames of $CH_4/NO_2/O_2$ and $CH_2O/NO_2/O_2$ Mixtures," *Combustion and Flame*, Vol. 83, Nos. 3 & 4, 1991, pp. 228–239.

[43]Vandooren, J., Branch, M. C., and Van Tiggelen, P. J., "Comparisons of the Structure of Stoichiometric CH_4-N_2O-Ar and CH_4-O_2-Ar Flames by Molecular Beam Sampling and Mass Spectrometric Analyses," *Combustion and Flame*, Vol. 90, Nos. 3 & 4, 1992, pp. 247–258.

[44]Dindi, H., Tsai, H.-M., and Branch, M. C., "Combustion Mechanism of Carbon Monoxide-Nitrous Oxide Flames," *Combustion and Flame*, Vol. 87, No. 1, 1991, pp. 13–20.

[45]Sausa, R. C., Anderson, W. R., Dayton, D. C., Faust, C. M., and Howard, S. L., "Detailed Structure Study of a Low Pressure, Stoichiometric H_2/N_2O/Ar Flame," *Combustion and Flame*, Vol. 94, No. 4, 1993, pp. 407–425.

[46]Howard, S. L., Sausa, R. C., Dayton, D. C., and Miziolek, A. W., "Mass Spectroscopic Studies of Propellant-Like Low-Pressure Flames," 28th JANNAF Combustion Subcommittee Meeting, San Antonio, TX, 1991.

[47]Dayton, D. C., Faust, C. M., Anderson, W. R., and Sausa, R. C., "Flame Structure Studies of a Lean H_2/N_2O/Ar Flame Employing

Molecular Beam Mass Spectrometry and Modeling," *Combustion and Flame*, Vol. 99, No. 2, 1994, pp. 323–330.

[48]Anderson, W. R., and Faust, C. M., "Modeling of H_2/N_2O Flames," 29th JANNAF Combustion Subcommittee Meeting, Hampton, VA, Nov. 1992.

[49]Thorne, L. R., and Melius, C. F., "The Structure of Hydrogen Cynanide-Nitrogen Dioxide Premixed Flames," 27th JANNAF Combustion Meeting, Nov. 1989.

[50]Cattolica, R., Smooke, M., and Dean, A., "A Hydrogen-Nitrous Oxide Flame Study," Fall Meeting of the Western States Section of the Combustion Inst., The Combustion Inst., Sandia National Labs., Livermore, CA, 1982.

[51]Miller, J. A., and Bowman, C. T., "Mechanism and Modeling of Nitrogen Chemistry in Combustion," *Progress in Energy and Combustion Science*, Vol. 15, No. 4, 1989, pp. 287–338.

[52]Vermeersch, M. L., Ph.D. Dissertation, Dept. of Mechanical and Aerospace Engineering, Princeton Univ., Princeton, NJ, 1991.

[53]Linteris, G., Yetter, R. A., Brezinsky, K., and Dryer, F. L., "Hydroxyl Radical Concentration Measurement in Carbon Monoxide in a Chemical Kinetic Flow Reactor," *Combustion and Flame*, Vol. 86, Nos. 1 & 2, 1991, pp. 162–170.

[54]Yetter, R. A., Dryer, F. L., and Rabitz, H., "Flow Reactor Studies of Carbon Monoxide/Hydrogen/Oxygen Kinetics," *Combustion Science and Technology*, Vol. 79, Nos. 1–3, 1989, pp. 129–140.

[55]Yetter, R. A., Eslava, L. A., Dryer, F. L., and Rabitz, H., "Elementary and Derived Sensitivity Information in Chemical Kinetics," *Journal of Physical Chemistry*, Vol. 88, No. 8, 1984, pp. 1497–1507.

[56]Yetter, R. A., Dryer, F. L., and Rabitz, H., "Some Interpretive Aspects of Elementary Sensitivity Gradients in Combustion Kinetics Modeling," *Combustion and Flame*, Vol. 59, No. 2, 1985, pp. 107–133.

[57]Yetter, R. A., Rabitz, H., Dryer, F. L., Klemm, R. B., and Maki, R. G., "Evaluation of the Rate Constant for the Reaction OH + H_2CO: Application of Modeling and Sensitivity Analysis Techniques for Determination of the Product Branching Ratio," *Journal of Chemical Physics*, Vol. 91, No. 7, 1989, pp. 4088–4097.

[58]Allen, M. T., Yetter, R. A., and Dryer, F. L., "The Thermal Decomposition of Nitrous Oxide at $1.5 < P < 10.5$ atm and $1103 < T < 1173$ K," *International Journal of Chemical Kinetics* (to be published).

[59]Davidson, D. F., DiRosa, M. D., Chang, A. Y., and Hanson, R. K., "Shock Tube Measurements of the Major Product Channels of N_2O + O," *Proceedings of the 18th International Symposium on Shock-Tube Waves*, edited by K. Takayama, Springer–Verlag, 1992, pp. 813–818.

[60]Baulch, D. L., Drysdale, D. D., Horne, D. G., and Lloyd, A. C., *Evaluated Kinetic Data for High Temperature Reactions*, Vols. 1 and 2, Butterworths, London, 1973.

[61]Kaufman, F., Gerri, N. J., and Bowman, R. E., "Role of Nitric Oxide in the Thermal Decomposition of Nitrous Oxide," *Journal of Chemical Physics*, Vol. 25, No. 1, 1956, pp. 106–115.

[62]Allen, M. T., Yetter, R. A., and Dryer, F. L., "The Oxidation of Carbon Monoxide by Nitrous Oxide," 31st JANNAF Subcommittee Meeting on Combustion, Sunnyvale, CA, Oct. 1994.

[63]Glarborg, P., and Dam-Johansen, K., "Thermal Decomposition of Nitrous Oxide," *Combustion and Flame*, Vol. 99, Nos. 3 & 4, 1994, pp. 523–532.

[64]Miller, J. A., Melius, C. F., and Durant, J. L., private communication, Sandia National Lab., Livermore, CA.

[65]Ross, S., Sutherland, J. W., and Klemm, R. B., private communication, Brookhaven National Lab., Upton, NY.

[66]Gatto, J. L., Yetter, R. A., and Dryer, F. L., "The Thermal Decomposition of Nitrogen Dioxide," Eastern States Section of the Combustion Inst., Clearwater, FL, Dec. 1994.

[67]Yetter, R. A., Ilincic, N., Dryer, F. L., Allen, M. T., and Gatto, J. L., "Kinetic Studies on Gas-Phase Reaction Mechanisms Important to the Combustion Process of High Energy Density Materials: The H_2/NO_2 Reaction," 29th JANNAF Combustion Subcommittee Meeting, Hampton, VA, Nov. 1992.

[68]Allen, M. T., Yetter, R. A., and Dryer, F. L., "Kinetic Studies on Gas-Phase Reaction Mechanisms Important to the Combustion Process of High Energy Density Materials: The Oxidation of Methane by Nitrous Oxide," 30th JANNAF Combustion Subcommittee Meeting, Monterey, CA, Nov. 1993.

[69]Tsang, W., "Chemical Kinetic Data Base for Propellant Combustion II. Reactions Involving CN, NCO, and HNCO," *Journal of Physical Chemistry, Reference Data*, Vol. 21, No. 4, 1992, pp. 753–791.

[70]Kim, T. J., Yetter, R. A., and Dryer, F. L., "New Results on Moist CO Oxidation: High Pressure, High Temperature Experiments and Comprehensive Kinetic Modeling," *25th Symposium (International) on Combustion*, The Combustion Inst., Pittsburgh, PA, 1994, pp. 759–766.

[71]Mishra, M., Yetter, R. A., Revren, Y., Rabitz, H., and Smooke, M., "On the Role of Transport on the Combustion Kinetics of a Steady-State Premixed Laminar $CO/H_2/O_2$ Flame," *International Journal of Chemical Kinetics*, Vol. 26, No. 4, 1994, pp. 437–454.

[72]Thaxton, A. G., Diau, E. X. G., Lin, M. C., Lin, C.-Y., and Melius, C. F., "Thermal Oxidation of HCN by NO_2 at High Temperatures," *International Journal of Chemical Kinetics* (submitted for publication).

[73]Yetter, R. A., Dryer, F. L., and Golden, D. M., "Pressure Effects on the Kinetics of High Speed Chemically Reacting Flows," *Major Topics in Combustion*, edited by M. Y. Hussani, A. Kumar, and R. G. Voight, ICASE/NASA Series, Springer–Verlag, New York, 1992, pp. 309–338.

[74]Melius, C. F., Bergan, N. E., and Shepherd, J. E., "Effects of Water on Combustion Kinetics at High Pressure," 23rd Symposium (International) on Combustion, The Combustion Inst., Pittsburgh, PA, 1990, pp. 217–223.